

CHANDRA DETECTION OF XTE J1650–500 IN QUIESCENCE AND THE MINIMUM LUMINOSITY OF BLACK HOLE X-RAY BINARIES

ELENA GALLO^{1,2}, JEROEN HOMAN³, PETER G. JONKER^{4,5}, JOHN A. TOMSICK⁶

Draft version October 31, 2018

ABSTRACT

The Galactic black hole X-ray binary XTE J1650–500 entered a quiescent regime following the decline from the 2001–2002 outburst that led to its discovery. Here we report on the first detection of its quiescent counterpart in a 36 ks observation taken in 2007 July with the *Chandra X-ray Observatory*. The inferred 0.5–10 keV unabsorbed flux is in the range $2.5\text{--}5.0 \times 10^{-15} \text{ erg s}^{-1} \text{ cm}^{-2}$. Notwithstanding large distance uncertainties, the measured luminosity is comparable to that of the faintest detected black hole X-ray binaries, all having orbital periods close to the expected bifurcation period between *j*- and *n*-driven low-mass X-ray binaries. This suggests that a few $10^{30} \text{ erg s}^{-1}$ might be a limiting luminosity value for quiescent black holes.

Subject headings: X-rays: binaries — accretion, accretion disks — black hole physics — stars: individual (XTE J1650–500)

1. INTRODUCTION

Black hole (BH) X-ray transients – close binary systems in which a low-mass donor transfers mass via Roche-lobe overflow onto a black hole accretor – spend most of their lifetimes in a low-luminosity state, where the boundary between ‘quiescence’ and more active regime can be set around $10^{33.5} \text{ erg s}^{-1}$, corresponding to a few 10^{-6} times the Eddington luminosity (L_{Edd}) for a $10 M_{\odot}$ object (e.g. McClintock & Remillard 2006). Broadly speaking, the low Eddington ratios can be due to low radiative efficiency or low net accretion rate in the inner regions, or a combination of the two (see e.g. Narayan 2005, and references therein). First explored in their basic ideas by Ichimaru (1977), and Rees et al. (1982), stable, radiatively inefficient accretion flow models were later formalized and gained vast popularity owing to the works of Narayan & Yi (1994, 1995), and Abramowicz et al. (1995). Since the mid 1990s, they have been widely employed to account for the broadband (radio/optical/UV/X-ray) spectra of low-luminosity BH candidates, such as A0620–00, GS 1124–68 and V404 Cyg (Narayan et al. 1996, 1997a), as well as the Galactic center source Sgr A* (Narayan et al. 1995). The increased sensitivity of *Chandra* and *XMM-Newton* with respect to previous X-ray telescopes has eventually permitted detailed X-ray studies of quiescent Galactic BHs down to Eddington ratios as low as a few 10^{-9} (Garcia et al. 2001; Kong et al. 2002; Hameury et al. 2003; Tomsick et al. 2003; McClintock et al. 2003; Gallo et al. 2006; Homan et al. 2006; Corbel et al. 2006; Bradley et al. 2007). In the framework of advection-dominated accretion flow models (ADAF; Narayan & Yi 1994, 1995), the observed luminosity difference between quiescent BHs and quiescent neutron stars – the former being fainter by about one order of magnitude at comparable

orbital periods – has been interpreted as evidence for the existence for an event horizon in BHs (Narayan et al. 1997b; Menou et al. 1999; Garcia et al. 2001; Narayan & McClintock 2008). At the same time, recent studies at lower frequencies, in the radio and mid-infrared bands, suggest that BHs and neutron stars may channel different fractions of the total accretion power into relativistic outflows, with a substantially reduced jet contribution in quiescent neutron stars with respect to BHs (Fender et al. 2003; Gallo et al. 2006, 2007; Migliari et al. 2006; Köerding et al. 2007).

Of the 40 candidate BH X-ray binaries⁷ listed by Remillard & McClintock (2006), 15 have sensitive measurements/upper limits on their quiescent X-ray luminosities. In this Letter, we report on a 36 ks observation of the quiescent BH XTE J1650–500 performed in 2007 July with the *Chandra X-ray Observatory*, and briefly discuss it in the context of quiescent BH X-ray binaries and how the advent of high sensitivity/resolution X-ray telescopes has improved our understanding of such systems.

The Galactic X-ray binary system XTE J1650–500 entered a quiescent regime following the 2001–2002 outburst that led to its discovery with the *Ross X-ray Timing Explorer* (Remillard 2001). Observations conducted with *XMM-Newton* and *BeppoSAX* in late 2001, right after the outburst peak, revealed a broad, asymmetric Fe K α emission line, interpreted as due to irradiation of the inner accretion disk around a rapidly spinning Kerr BH (Miller et al. 2002; Miniutti et al. 2004; see Done & Gierlinski 2006 for a different interpretation). The prolonged quiescent regime has allowed for the derivation of the system orbital period and optical mass function: $P_{\text{orb}}=7.7 \text{ hr}$, and $f(M)=2.73\pm0.56 M_{\odot}$, respectively (Orosz et al. 2004). The mass of the BH in XTE J1650–500 is highly uncertain. The amplitude of the phased *R*-band light curve results in a lower bound to the orbital inclination $i > 50^{\circ}\pm3^{\circ}$, which, in the limiting case of no disk contribution, implies in an upper limit of $7.3 M_{\odot}$ to the accretor mass (Orosz et al. 2004). However –caveat the poor signal-to-noise of the adopted stellar templates– these authors find that the accretion disk contribution in the *R* band can be as high as $\gtrsim 80\%$.

⁷ Additional likely BH candidates have been since discovered, including: XTE J1817–330, Swift J1753.5–0127, IGR J17091–3624, IGR J17098–3628, IGR J17497–2821 and IGR J18539+0727.

¹ Physics Department, Broida Hall, University of California Santa Barbara, CA 93106

² Chandra Fellow

³ Kavli Institute for Astrophysics and Space Research, Massachusetts Institute of Technology, 77 Massachusetts Av., Cambridge, MA 02139

⁴ SRON, Netherlands Institute for Space Research, Sorbonnelaan 2, 3584 CA, Utrecht, NL

⁵ Harvard-Smithsonian Center for Astrophysics, 60 Garden Street, Cambridge, MA 02138

⁶ Space Sciences Laboratory, 7 Gauss Way, University of California Berkeley, CA 94720

This results in an orbital inclination $i = 70^\circ$ or higher, that is a mass of only $4 M_\odot$ for the BH.

The non-detection of XTE J1650–500 with *XMM-Newton*, in 2005 March, yielded an upper limit on its quiescent unabsorbed flux of $1.1\text{--}1.3 \times 10^{-14} \text{ erg s}^{-1} \text{ cm}^{-2}$ (0.5–10 keV), depending on the assumed spectral model (Homan et al. 2006). At a (by no means certain⁸) distance of 2.6 kpc, this corresponds to a X-ray luminosity $L_X \lesssim 10^{31} \text{ erg s}^{-1}$, comparable to the lowest luminosities inferred for quiescent BH X-ray binaries (i.e. GRO J1655–40, GRO J0422+32, XTE J1118+480, A0620–00 and GS 2000+25).

2. OBSERVATION AND DATA ANALYSIS

The field of view of XTE J1650–500 was observed with the Advanced CCD Imaging Spectrometer (ACIS) detector on board *Chandra* on 2007 June 30 at 23:46 UT for approximately 36 ks. The target was placed on the back-side illuminated S3 chip in order to take advantage of the detector sensitivity to low-energy X-rays. The data were telemetered in very faint (VF) mode with an upper energy cut-off at 13 keV, in order to minimize the chances of saturation. We have reprocessed and analyzed the data using the *Chandra* Interactive Analysis Observation (CIAO) software version 3.4.1.1. The level 1 event lists were first cleaned following the standard threads to reduce the ACIS particle background for VF mode observations, including only ASCA grades 0,2,3,4 and 6. Further analysis was restricted between 0.3–7.0 keV in order to avoid calibration uncertainties at low energies and to limit background contaminations at high energies. As *Chandra* is known to encounter periods of high background, which especially affect the S1 and S3 chips, we first checked for background flares but found none, resulting in a net exposure of 35.65 ks. We applied a wavelet detection algorithm, using CIAO *wavdetect* with a sensitivity threshold that corresponds to a 3.8×10^{-6} chance of detecting a spurious source per point spread function (PSF) element if the local background is uniformly distributed. We employed the default ‘Mexican Hat’ wavelet, with scales increasing by a factor of $\sqrt{2}$ between 1–16 pixels on a full resolution circular region of 512 pixel radius centered on the nominal position of the target (restricting the circle to the S3 chip). Table 1 lists the 28 sources detected by the algorithm, in order of increasing count rate (the positions were obtained after registering the *Chandra* image to the USNO B1 catalog, see below). Three of the detected X-ray sources have optical counterparts with positions listed in the US Naval Observatory (USNO) B1 catalog (Monet et al. 2003), which has an absolute positional error of $0''.20$. The mean USNO to *Chandra* shifts in right ascension α and declination δ are $0''.06 \pm 0''.31$ and $0''.08 \pm 0''.31$, respectively, where the uncertainties account for the *Chandra* statistical errors as well as the USNO B1 positional uncertainty. We thus registered the *Chandra* image by applying the above astrometric corrections, and ran *wavdetect* again on the registered image to obtain refined position of the X-ray sources.

The position of source 3, shown in Figure 1, is consistent with the X-ray position of XTE J1650–500 reported by Tomsick et al. (2004) based on *Chandra* observations taken during

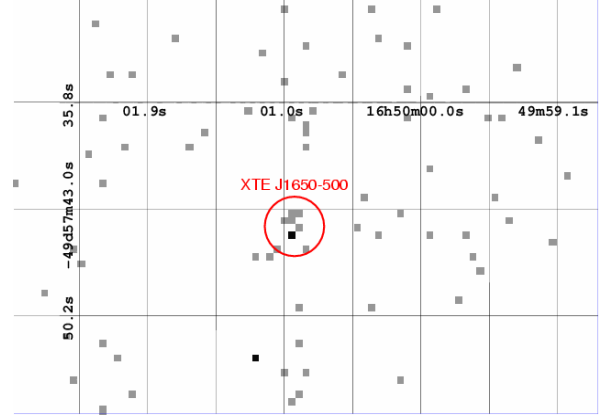


FIG. 1.— *Chandra* image of the field around XTE J1650–500 (ACIS-S3, 0.3–7 keV). The red circle – centered on the source position as identified by the CIAO *wavdetect* – marks the count extraction region. The astrometry has been improved by cross-matching the *Chandra* image to the USNO B1 catalog; the revised *Chandra* position of XTE J1650–500 is: R.A.: $16^{\text{h}}:50^{\text{m}}:00^{\text{s}}.92$, decl.: $-49^{\circ}:57':44''.1$ (J2000.0), with an uncertainty of $0''.31$. For reference, 1 pixel corresponds to $0''.492$. North is at the top and East is on the left on this image.

a higher luminosity state: after the astrometric correction, the revised position of XTE J1650–500 is: $\alpha=16^{\text{h}}:50^{\text{m}}:00^{\text{s}}.92$, $\delta=-49^{\circ}:57':44''.1$ (equinox J2000.0), with an uncertainty of $0''.31$. In order to determine the optimal extraction region for the source counts, we generated the ACIS PSF at 1.5 keV at the position of XTE J1650–500, and (arbitrarily) normalized it to 10^4 counts. This allows for an evaluation of $R_{95\%}$, the radius which encircles 95% of the energy; At this angular off-set ($0'.302$), $R_{95\%}=2''$ at 1.5 keV. A total of 9 counts are measured within a circle with $2''$ radius centered on the position of XTE J1650–500 given above. The inferred number of *net* counts is 8.2 ± 2.9 . In order to quantify the significance of the detection, we compared the total number of counts within a $2''$ radius circular aperture, and within a background annulus with inner and outer radii $R_{\text{in}}=5''$ and $R_{\text{out}}=25''$, both centered on the target position. We found 9 counts within the $2''$ radius aperture, and 122 counts within the background annulus. The Poisson probability of obtaining 9 counts or more when 0.8 are expected is $\sim 2 \times 10^{-7}$, implying a detection at the 99.99998% confidence level (e.g. Weisskopf et al. 2007). The low number of counts detected from XTE J1650–500 does not allow for a proper spectral modeling. We estimated an approximate flux using webPIMMS⁹. Assuming an absorbed power law model with photon index $\Gamma = 1.7 - 2$ (typical for quiescent BHs, e.g. Corbel et al. 2006) and equivalent hydrogen column $N_{\text{H}} = 6.7 \times 10^{21} \text{ cm}^{-2}$ (Tomsick et al. 2004), the measured net count rate of $2.3 \pm 0.8 \times 10^{-4} \text{ cps}$ results in an unabsorbed flux $F_X = 3.7 \pm 1.3 \times 10^{-15} \text{ erg s}^{-1} \text{ cm}^{-2}$ over the energy interval 0.5–10.0 keV (the quoted flux uncertainty accounts for both counting statistics and the different assumed spectral shapes, being dominated by the former). This yields a luminosity $L_X \simeq 3 \pm 1 \times 10^{30} (D/2.6 \text{ kpc})^2 \text{ erg s}^{-1}$ over the same energy interval, well below the upper limit from *XMM-Newton* (Homan et al. 2006). We wish to stress once again the large uncertainty in the distance, whose estimation method in turn relies on the uncertain BH mass value (see Appendix in Homan et al. 2006). For a maximum BH mass of $7.3 M_\odot$,

⁸ Similarly to its mass, the distance to XTE J1650–500 is also uncertain: the quoted value was estimated by Homan et al. (2006) based on the system Eddington-scaled X-ray luminosity at the soft-to-hard X-ray state transition, following Maccarone & Coppi (2003). As such, it suffers from uncertainties of at least a factor 2.

⁹ <http://heasarc.nasa.gov/Tools/w3pimms.html>

TABLE 1
Chandra DETECTED SOURCES IN THE XTE J1650–500 FIELD.

Source (1)	Name (2)	R.A. (3)	Decl. (4)	Count rate (5)	Notes (6)
1	CXOU J165007.6-495623	16 50 07.69	-49 56 23.8	1.9 (0.7)	
2	CXOU J165000.2-495723	16 50 00.21	-49 57 23.4	1.9 (0.7)	
3	XTE J1650-500	16 50 00.92	-49 57 44.1	2.0 (0.7)	
4	CXOU J165006.3-495814	16 50 06.37	-49 58 14.3	2.0 (0.7)	
5	CXOU J165013.1-495709	16 50 13.14	-49 57 09.1	2.0 (0.7)	
6	CXOU J165005.4-495427	16 50 05.48	-49 54 27.6	2.1 (0.8)	
7	CXOU J165002.5-495333	16 50 02.56	-49 53 34.0	2.2 (0.8)	
8	CXOU J164943.9-495901	16 49 43.97	-49 59 01.3	2.2 (0.8)	
9	CXOU J165012.1-495715	16 50 12.12	-49 57 15.2	2.4 (0.8)	
10	CXOU J165000.3-495655	16 50 00.38	-49 56 55.9	2.5 (0.8)	
11	CXOU J165006.0-495455	16 50 06.05	-49 54 55.1	2.5 (0.8)	USNO B1
12	CXOU J165021.3-495632	16 50 21.38	-49 56 32.0	3.0 (0.9)	
13	CXOU J164950.3-495931	16 49 50.30	-49 59 31.0	3.1 (0.9)	
14	CXOU J165006.3-495743	16 50 06.35	-49 57 44.0	3.6 (1.0)	
15	CXOU J165009.1-495442	16 50 09.10	-49 54 42.9	4.2 (1.1)	USNO B1
16	CXOU J164959.7-495518	16 49 59.77	-49 55 18.7	4.2 (1.1)	
17	CXOU J164958.5-495614	16 49 58.54	-49 56 14.2	4.8 (1.2)	
18	CXOU J164951.8-495653	16 49 51.87	-49 56 53.8	5.2 (1.2)	
19	CXOU J165013.9-495726	16 50 13.94	-49 57 26.7	5.3 (1.2)	
20	CXOU J164947.8-500119	16 49 47.82	-50 01 19.9	5.4 (1.2)	
21	CXOU J164955.5-495705	16 49 55.50	-49 57 05.6	5.6 (1.2)	
22	CXOU J165005.2-495622	16 50 05.27	-49 56 22.6	5.9 (1.3)	
23	CXOU J164943.2-495450	16 49 43.28	-49 54 50.6	7.2 (1.4)	
24	CXOU J165005.1-495624	16 50 05.13	-49 56 24.3	7.2 (1.4)	USNO B1
25	CXOU J164956.0-495711	16 49 56.04	-49 57 11.2	8.0 (1.5)	
26	CXOU J164953.5-495747	16 49 53.59	-49 57 47.6	8.6 (1.5)	
27	CXOU J164948.8-495509	16 49 48.82	-49 55 09.8	9.4 (1.6)	
28	CXOU J164948.7-495936	16 49 48.72	-49 59 36.2	11.5 (1.8)	

NOTE. — (1) Target numeration (2) Source name following the *Chandra* convention (3) Units of right ascension (equinox J2000.0) are hours, minutes, seconds; (4) Units of declination (equinox J2000.0) are degrees, arcminutes and arcseconds; (5) Net count rate, in units of 10^{-4} cps, as measured by *wavdetect*, with errors given in parenthesis, over the energy interval 0.3–7.0 keV. Notice that *wavdetect* is designed to be used as a detection algorithm, and only secondarily as a source flux measurement tool. Count rates are generally reliable, but can be slightly under-estimated for very low number of counts.

the inferred luminosity corresponds to a minimum Eddington-scaled luminosity $L_X \gtrsim 3 \times 10^{-9} L_{\text{Edd}}$ (Orosz et al. 2004).

3. DISCUSSION

As illustrated in Figure 2 (updated from Tomsick et al. 2003 after Corbel et al. 2006, Gallo et al. 2006 and Homan et al. 2006), the quiescent X-ray luminosity of XTE J1650–500 as measured by *Chandra* sits in the range of values inferred for systems with similar orbital periods. Out of 15 candidate BH X-ray binary systems with sensitive observations while in the quiescent regime, 12 have now been detected in X-rays. For those 12, the quiescent luminosities range between a few 10^{30} and 10^{33} erg s $^{-1}$. The nearest BH, A0620–00, has been steadily emitting at $\simeq 2-3 \times 10^{30}$ erg s $^{-1}$ at least for the past 5 years (Kong et al. 2002; Gallo et al. 2006); this is approximately the same luminosity level as XTE J1650–500 (this work), XTE J1118+480 (McClintock et al. 2003) and GS 2000+25 (Garcia et al. 2001), suggesting that this might be some kind of limiting value.

Indeed, for low-mass X-ray binaries one can make use of binary evolution theory, combined with a given accretion flow solution, to predict a relation between the minimum quiescent luminosity and the system orbital period P_{orb} (see e.g. Menou et al. 1999; Lasota 2000). As an example, Figure 4 of Menou et al. (1999) illustrates how the predicted luminosity of quiescent BHs powered by ADAFs depends on the ratio between the outer mass transfer rate and the ADAF accretion rate. The lower band, which roughly reproduces the observed luminosities of 3 representative systems spanning the whole range of

detected luminosities (A0620–00, GRO J1655–40 and V404 Cyg), corresponds to $\sim 1/3$ of the mass transferred being accreted via the ADAF, whereas the remaining 2/3 would be either accumulated in an outer thin disk or lost to an outflow. Most importantly, independently of the actual solution for the accretion flow in quiescence, the existence of a minimum luminosity in low-mass X-ray binaries stems directly from the existence of a bifurcation period, P_{bif} , below which the mass transfer rate is driven by gravitational wave radiation (j -driven systems), and above which it is dominated by the nuclear evolution of the secondary star (n -driven systems). Specifically, the outer mass transfer rate \dot{M}_T increases with decreasing orbital period below P_{bif} , while increases with increasing orbital period above P_{bif} (the same applies to quiescent neutron star X-ray binaries, although with higher normalization). For a wide range of donor masses, Menou et al. find $P_{\text{bif}} \simeq 10$ hr. As long as the luminosity expected from a given accretion flow model scales with a positive power of \dot{M}_T , systems with orbital periods close to the bifurcation period should display the lowest quiescent luminosities. Caveat the large distance uncertainties which affect most BH X-ray binaries (e.g. Jonker & Nelemans 2004), this is indeed observed, as illustrated in the right panel of Figure 2.

Deep observations of short ($\lesssim 5$ hr), as well as long ($\gtrsim 200$ hr) orbital period systems will hopefully add to the slim statistics in support of this argument. We wish to point out that, given the distance/absorption column to the 3 BH systems with upper limits (H1705–250, GRS1009–45 and 4U 1543–47; see Figure 2), several tens of ks of integra-

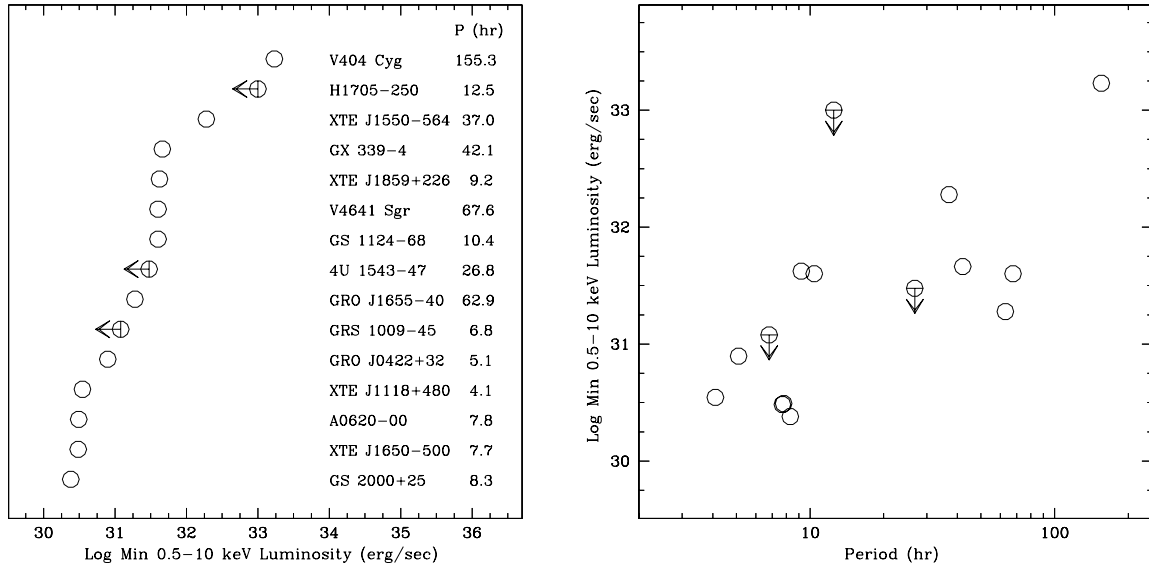


FIG. 2.— *Left*: Quiescent X-ray luminosities/upper limits for 15 BH X-ray binaries with sensitive observations (down to a minimum threshold of $\sim 10^{33.5}$ erg s $^{-1}$). *Right*: The measured luminosities are plotted against the systems' orbital periods. The faintest systems (GS 2000+25, A0620–00 and XTE J1650–500) have orbital periods close to 10 hr, the expected bifurcation period between j - and n -driven low-mass X-ray binaries according to Menou et al. (1999).

tion with *Chandra* would be needed in order to detect them, should their luminosity be close to that of the faintest objects. Quiescent ultra-compact X-ray binaries (with orbital periods $P_{\text{orb}} \lesssim 1$ hr) could be primary targets to test this conclusion at the short P_{orb} end. However, the argument has been made that the mass-transfer rate evolution has not been studied in any detail for systems with such very low mass ratios. Extreme mass ratios could result in a drastically reduced \dot{M}_T , making the direct comparison between quiescent ultra-compact and longer period binaries somewhat dubious (see Jonker et al. 2006, 2007, and related discussion in Lasota 2007). For long orbital period systems, the ideal testbed would be obviously provided by the power off of the as yet super-luminous GRS 1915+105, with an orbital period of over

800 hr. Similarly, the newly discovered BH candidate Swift J1753.5–0127, with an inferred orbital period of 3.2 hr (Zurita et al. 2008), represents the ideal short period target.

E.G. is funded by NASA through *Chandra* Postdoctoral Fellowship grant number PF5-60037, issued by the *Chandra* X-ray Observatory Center, which is operated by the Smithsonian Astrophysical Observatory for NASA under contract NAS8-03060. Support for this work was provided through *Chandra* Award Number G07-8047A issued by the *Chandra* X-ray Observatory Center. We wish to thank the referee for a prompt and thoughtful report.

REFERENCES

- Abramowicz, M. A., Chen, X., Kato, S., Lasota, J.-P., & Regev, O. 1995, *ApJ*, 438, L37
- Bradley, C. K., Hynes, R. I., Kong, A. K. H., Haswell, C. A., Casares, J., & Gallo, E. 2007, *ApJ*, 667, 427
- Corbel, S., Fender, R. P., Tomsick, J. A., Tzioumis, A. K., & Tingay, S. 2004, *ApJ*, 617, 1272
- Done, C., & Gierlinski, M. 2006, *MNRAS*, 367, 659
- Fender R. P., Gallo E., & Jonker P. G. 2003, *MNRAS*, 343, L99
- Gallo, E., Migliari, S., Markoff, S., Tomsick, J. A., Bailyn, C. D., Berta, S., Fender, R., & Miller-Jones, J. C. A. 2007, *ApJ*, 670, 600
- Gallo, E., Fender, R. P., Miller-Jones, J. C. A., Merloni, A., Jonker, P. G., Heinz, S., Maccarone, T. J., & van der Klis, M. 2006, *MNRAS*, 370, 1351
- Garcia, M. R., McClintock, J. E., Narayan, R., Callanan, P., Barret, D., & Murray, S. S. 2001, *ApJ*, 553, L47
- Hameury, J.-M., Barret, D., Lasota, J.-P., McClintock, J. E., Menou, K., Motch, C., Olive, J.-F., & Webb, N. 2003, *A&A*, 399, 631
- Homan, J., Wijnands, R., Kong, A., Miller, J. M., Rossi, S., Belloni, T., & Lewin, W. H. G. 2006, *MNRAS*, 366, 235
- Ichimaru, S. 1977, *ApJ*, 214, 840
- Jonker, P. G., Steeghs, D., Chakrabarty, D., & Juett, A. M. 2007, *ApJ*, 665, L147
- Jonker, P. G., Bassa, C. G., Nelemans, G., Juett, A. M., Brown, E. F., & Chakrabarty, D. 2006, *MNRAS*, 368, 1803
- Jonker, P. G. & Nelemans, G. 2004, *MNRAS*, 354, 355
- Kong, A. K. H., McClintock, J. E., Garcia, M. R., Murray, S. S., & Barret, D. 2002, *ApJ*, 570, 277
- Körding, E. G., Migliari, S., Fender, R., Belloni, T., Knigge, C., & McHardy, I. 2007, *MNRAS*, 380, 301
- Lasota, J.-P. 2007, *Comptes Rendus Physique*, 8, 45
- Lasota, J.-P. 2000, *A&A*, 360, 575
- Maccarone, T. J., & Coppi, P. S. 2003, *MNRAS*, 338, 189
- McClintock, J. E., & Remillard, R. A. 2006, in *Compact Stellar X-ray Sources*, ed. W. Lewin & M. van der Klis (Cambridge Univ. Press) 157
- McClintock, J. E., Narayan, R., Garcia, M. R., Orosz, J. A., Remillard, R. A., & Murray, S. S. 2003, *ApJ*, 593, 435
- Menou, K., Esin, A. A., Narayan, R., Garcia, M. R., Lasota, J.-P., & McClintock, J. E. 1999, *ApJ*, 520, 276
- Migliari, S., Tomsick, J. A., Maccarone, T. J., Gallo, E., Fender, R. P., Nelemans, G., & Russell, D. M. 2006, *ApJ*, 643, L41
- Miller, J. M., et al. 2002, *ApJ*, 570, L69
- Miniutti, G., Fabian, A. C., & Miller, J. M. 2004, *MNRAS*, 351, 466
- Monet, D. G., et al. 2003, *AJ*, 125, 984
- Narayan, R., & McClintock, J. E. 2008, *ArXiv e-prints*, 803.0322
- Narayan, R. 2005, *A&SS*, 300, 177
- Narayan, R., Barret, D., & McClintock, J. E. 1997a, *ApJ*, 482, 448
- Narayan, R., Garcia, M. R., & McClintock, J. E. 1997b, *ApJ*, 478, L79
- Narayan, R., McClintock, J. E., & Yi, I. 1996, *ApJ*, 457, 821
- Narayan, R. & Yi, I. 1995, *ApJ*, 452, 710
- Narayan, R., Yi, I., & Mahadevan, R. 1995, *Nature*, 374, 623
- Narayan, R., & Yi, I. 1994, *ApJ*, 428, L13
- Orosz, J. A., McClintock, J. E., Remillard, R. A., & Corbel, S. 2004, *ApJ*, 616, 376

Rees, M. J., Begelman, M. C., Blandford, R. D., & Phinney, E. S. 1984
Nature, 295, 17
Remillard, R. A., & McClintock, J. E. 2006, ARA&A, 44, 49
Remillard, R. 2001, IAU Circ., 7707
Tomsick, J. A., Kalemci, E., & Kaaret, P. 2004, ApJ, 601, 439
Tomsick, J. A., et al. 2003, ApJ, 597, L133

Weisskopf, M. C., Karovska, M., Pavlov, G. G., Zavlin, V. E., & Clarke, T.
2007, Ap&SS, 308, 151
Zurita, C., Durant, M., Torres, M. A. P., Shahbaz, T., Casares, J., & Steeghs,
D. 2008, ArXiv e-prints, 803.2524